Importance of individual scattering matrix elements at Fano resonances

2006 J. Phys.: Condens. Matter 18 5313

(http://iopscience.iop.org/0953-8984/18/23/005)

INSTITUTE OF PHYSICS PUBLISHING JOURNAL OF PHYSICS: CONDENSED MATTER

J. Phys.: Condens. Matter **18** (2006) 5313–5321 doi:10.1088/0953-8984/18/23/005

Importance of individual scattering matrix elements at Fano resonances

P Singha Deo[1] **and M Manninen**[2]

[1] Unit for Nanoscience and Technology, S N Bose National Centre for Basic Sciences, JD Block, Sector III, Salt Lake City, Kolkata 98, India
[2] Nanoscience Center, Department of Physics, University of Jyväskylä, PO Box 35, 40014 Jyväskylä, Finland

Received 6 February 2006, in final form 24 April 2006
Published 26 May 2006
Online at stacks.iop.org/JPhysCM/18/5313

Abstract

Single particle resonances in quantum wires are generally Fano resonances. In the case of Fano resonances, the scattering phase shift in some channels shows sharp phase drops and that in the other channels does not. The phase shift in a particular channel can be measured and can yield information about the integrated charge localized around the scatterer. This paper tries to analyse whether some channels are more informative than others, so that an experimentalist can measure the phase shift in only those channels. The paper also shows how to deal with non-trivial interpretation of density of states 'in the absence of scattering' in the case of scattering by topological defects.

1. Introduction

Miniaturization of devices eventually leads to systems that are so small that the laws of physics are determined by quantum mechanics, and understanding the properties of so-called mesoscopic systems becomes demanding [1]. Circuits of future devices will be made up of quantum wires. Junctions in such circuits also have to be understood from the perspective of quantum mechanics. Perhaps the simplest such junction is what is referred to as a three-prong potential [2] which is schematically shown in figure 1. There are several papers that explore the importance of such a junction in mesoscopic systems [3–5].

Recently, the phase shifts and resonances for such a three-prong geometry were measured by Kobayashi *et al* [6, 7]. Such resonances in a three-prong structure have also attracted some theoretical interest [8–10]. While in our case the resonances or quasi-bound states are created by applying the potential V (see figure 1), in the experimental set up of Kobayashi *et al*, the resonances are created by applying suitable gate voltages at certain places of the three-prong potential that allow them to continuously switch between a ring geometry and a three-prong geometry.

While bound states (or quasi-bound states) are important in understanding the thermodynamic properties of a sample [11], the scattering states are important in understanding the transport properties [12]. However, it is not always necessary to solve the bound states and

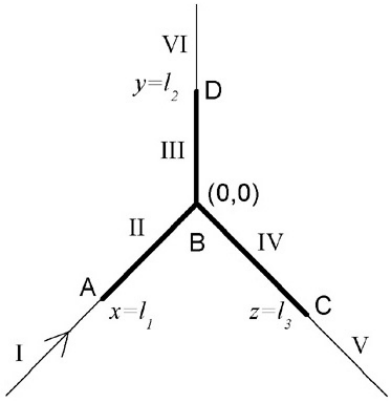

Figure 1. A schematic diagram of the system studied. Three semi-infinite quantum wires meet at a point B. In the thin regions the quantum mechanical potential V is zero but in the thick regions it is not zero. The arrow shows the direction of propagation of an incident electron.

the scattering states separately. Both these states are solutions of the same Hamiltonian but with different boundary conditions. It is possible to solve only the scattering states and thereby also understand the bound states as an analytical continuation of the scattering states. At the heart of this principle is the Friedel sum rule [13, 14] that states that for non-polarizable leads [13]

$$\frac{\mathrm{d}\theta_\mathrm{f}}{\mathrm{d}E} \approx \pi[\rho(E) - \rho_0(E)]. \tag{1}$$

Here

$$\theta_\mathrm{f} = \frac{1}{2\mathrm{i}} \log \mathrm{Det}[S], \tag{2}$$

E is the incident electron energy, S is the scattering matrix, $\rho(E)$ is the density of states (DOS) at energy E in the presence of scattering, and $\rho_0(E)$ is the DOS in the absence of scattering. θ_f is referred to as the Friedel phase. The RHS of equation (1) is therefore related to the integrated charge localized around the scatterer and this can be determined from the S matrix. The correction terms of equation (1) are small in the Wentzel–Kramers–Brillouin (WKB) regime [13].

A number of experiments [6, 7, 15] have shown that the phase of a particular scattering matrix element can be measured. Yeyati and Buttiker [16] first proposed that such phases can be understood from the Friedel sum rule (FSR). It was later found that transmission zeros play a special role [3, 9, 17, 18] and change our understanding of the FSR. Transmission zeros are also called antiresonances. While they were studied for Aharnov–Bohm rings [19], their occurrence in Fano resonances in mesoscopic quantum wires with defects is rather subtle although there is the same underlying principle and they belong to the same class [20]. While the line shapes of the Fano resonances were generalized [21], the universal features of the scattering phase shifts at Fano resonances have recently attracted attention [3, 17, 22]. It is worthwhile mentioning that Fano resonances are not just of interest in mesoscopic systems but are observed in many different areas [23].

2. The problem

Normally, in mesoscopic systems, S is a large but finite matrix, and often all the matrix elements are not completely independent. So, it may not be necessary to evaluate all the elements

of S, in order to calculate θ_f. Moreover, in mesoscopic systems, it is possible to measure a particular matrix element of S. One can measure the phase as well as the amplitude of the matrix element [15]. For a large-dimensional S matrix, it may not be possible to measure all the elements of S. So, it is important to know what kind of physical information can be obtained from the phase of a particular matrix element and which are the important matrix elements. For example, in the case of a strictly one-dimensional (1D) system, the scattering matrix is 2×2, and [24]

$$\frac{\mathrm{d}}{\mathrm{d}E} \arg(T) = \frac{\mathrm{d}\theta_f}{\mathrm{d}E} \tag{3}$$

where T is the transmission amplitude and $\arg(T) = \arctan(\mathrm{Im}[T]/\mathrm{Re}[T])$. The situation is complicated in quasi-1D where a single transverse mode is populated and the scattering matrix is 2×2. This is because of the presence of discontinuous changes in scattering phase shifts at Fano resonances [3]. Such a system was studied in [14, 25], which is somewhat similar to the system studied in this work and shown in figure 1. The difference is the absence of the lead at point D and imposing a hard wall boundary condition at point D. As a result the S matrix becomes 2×2. For such systems it was shown [14] that

$$\frac{\mathrm{d}}{\mathrm{d}E} \arg(T) = \frac{\mathrm{d}\theta_f}{\mathrm{d}E} \pm \pi\delta(E - E_0). \tag{4}$$

Here, E_0 is the (Fermi) energy at which $T = 0$. $T = 0$ occurs because of Fano resonance and is a general feature of quasi-1D [17]. The situation is further complicated in multichannel quasi-1D where the dimensionality of the S matrix is more than 2×2. In the case of a multichannel Fano resonance, there are sharp continuous phase drops at the minima of certain scattering probabilities, while not so for others [13]. For example, in the case of the δ function potential in a multichannel quantum wire, there are sharp drops in $\arg(T_{mm})$ versus incident energy, when $|T_{mm}|^2$ is minimum. But, this does not happen for $\arg(T_{mn})$ or $\arg(R_{mn})$ or $\arg(R_{mm})$. There it was shown that when $m \neq n$ [13]

$$\frac{\mathrm{d}}{\mathrm{d}E} \arg(R_{mn}) = \frac{\mathrm{d}}{\mathrm{d}E} \arg(R_{mm}) = \frac{\mathrm{d}}{\mathrm{d}E} \arg(T_{mn}) = \frac{\mathrm{d}\theta_f}{\mathrm{d}E} \tag{5}$$

where R_{mn} and T_{mn} are the reflection and transmission amplitudes from mth transverse channel to the nth transverse channel, respectively, and R_{mm} is the reflection amplitude from the mth transverse channel to mth transverse channel. Equation (5) is more general than equation (4). It is applicable also to the potentials studied in [14] (described above) while equation (4) does not apply to a multichannel wire with a δ function potential.

Equation (5) basically means that, for the systems studied in [13, 14], the integrated charge is determined by the energy derivatives of those $\arg(S_{\alpha\beta})$ that do not show a drop. Their derivatives are identical to the derivatives of the Friedel phase θ_f. However, the δ function potential, as well as the potentials studied in [14], are all point scatterers and it is not known if this feature is general. This motivates us to study an extended potential that can exhibit multichannel Fano resonance.

So in this paper we study the system shown in figure 1, as it is an extended potential. We shall show that it can exhibit multichannel Fano resonance. It is a simple model, that allows analytical understanding and allows us to check if the S matrix elements whose phase does not show a negative slope carry the information about the DOS. Besides, the potential considered here has certain subtleties. The subtlety arises with the interpretation of ρ_0, as will be explained in section 4.

3. The scattering solution

Consider the geometry, schematically shown in figure 1. The thin lines are semi-infinite 1D quantum wires with quantum mechanical potential $V = 0$, while the thick lines are quantum wires with a potential $V \neq 0$. An incident electron is shown by the arrow head and the quantum mechanical wavefunctions in the different regions I, II, III, IV, V and VI are written below.

$$\psi_{\mathrm{I}} = \mathrm{e}^{\mathrm{i}k(x-l_1)} + R_{11}\mathrm{e}^{-\mathrm{i}k(x-l_1)} \tag{6}$$

$$\psi_{\mathrm{II}} = A\mathrm{e}^{\mathrm{i}qx} + B\mathrm{e}^{-\mathrm{i}qx} \tag{7}$$

$$\psi_{\mathrm{III}} = C\mathrm{e}^{\mathrm{i}qy} + D\mathrm{e}^{-\mathrm{i}qy} \tag{8}$$

$$\psi_{\mathrm{IV}} = F\mathrm{e}^{\mathrm{i}qz} + G\mathrm{e}^{-\mathrm{i}qz} \tag{9}$$

$$\psi_{\mathrm{V}} = T_{13}\mathrm{e}^{\mathrm{i}k(z-l_3)} \tag{10}$$

$$\psi_{\mathrm{VI}} = T_{12}\mathrm{e}^{\mathrm{i}k(y-l_2)} \tag{11}$$

l_1, l_2 and l_3 are defined in figure 1. These wavefunctions have to be continuous and current has to be conserved at the junctions. From this we get a set of nine linear equations from which we can solve the nine unknown coefficients, i.e., A, B, C, D, F, G, R_{11}, T_{12} and T_{13}. Similarly, we have to solve the scattering problem when the incident electron comes from the top, in order to obtain R_{22}, T_{21}, etc. Thus we can determine the scattering matrix. It is a three-channel problem and the scattering matrix is 3×3, as shown below.

$$S = \begin{pmatrix} R_{11} & T_{12} & T_{13} \\ T_{21} & R_{22} & T_{23} \\ T_{31} & T_{32} & R_{33} \end{pmatrix}. \tag{12}$$

The definition of local density of states (LDOS) can be seen from text books [1]:

$$\rho(E) = -\frac{1}{\pi}\mathrm{Im}\,\mathrm{Tr}[G^{\mathrm{ret}}(r, r', E)] = \sum_{k,l}\delta(E - E_{k,l})\int_{-\infty}^{\infty}\mathrm{d}r|\psi_{k,l}(r)|^2.$$

Here $G^{\mathrm{ret}}(r, r', E)$ is the retarded Green's function. Allowed modes in the system are denoted by momentum index $k = \sqrt{2m(E - V)/\hbar^2}$ and l can take three values (1, 2 and 3), corresponding to an incident electron from three possible directions. Here m is the electronic mass and $v = \hbar k/m$. Starting from this definition we have found

$$\rho(E) = \rho^{(W)}(E) + \frac{2}{hv}\int_{-\infty}^{l_1}\mathrm{d}x + \frac{2}{hv}\int_{l_2}^{\infty}\mathrm{d}y + \frac{2}{hv}\int_{l_3}^{\infty}\mathrm{d}z + \frac{2|R_{11}|}{hv}\int_{-\infty}^{l_1}\cos(2kx + \eta_1)\,\mathrm{d}x$$
$$+ \frac{2|R_{22}|}{hv}\int_{-\infty}^{l_2}\cos(2ky + \eta_2)\,\mathrm{d}y + \frac{2|R_{33}|}{hv}\int_{-\infty}^{l_3}\cos(2kz + \eta_3)\,\mathrm{d}z \tag{13}$$

where $\rho^{(W)}(E)$ is the integrated local DOS in the thick region of figure 1, $\eta_1 = -\arg(R_{11})$, and so on. Here

$$\rho^{(W)}(E) = \rho_1^{(W)}(E) + \rho_2^{(W)}(E) + \rho_3^{(W)}(E) = \sum_l \rho_l^{(W)}(E) \tag{14}$$

where, for example,

$$\rho_1^{(W)}(E) = \frac{1}{hv}\left[\int_{l_1}^{0}|A\mathrm{e}^{\mathrm{i}qx} + B\mathrm{e}^{-\mathrm{i}qx}|^2\,\mathrm{d}x\right.$$
$$\left. + \int_0^{l_2}|C\mathrm{e}^{\mathrm{i}qy} + D\mathrm{e}^{-\mathrm{i}qy}|^2\,\mathrm{d}y + \int_0^{l_3}|F\mathrm{e}^{\mathrm{i}qz} + G\mathrm{e}^{-\mathrm{i}qz}|^2\,\mathrm{d}z\right] \tag{15}$$

and the others are similar, but the coefficients differ due to different boundary conditions. That is, $\rho_1^{(W)}(E)$ is calculated with the incident electron from the left, $\rho_2^{(W)}(E)$ is calculated with

the incident electron from the top, and $\rho_3^{(W)}(E)$ is calculated with the incident electron from the right. Substituting equation (13) in equation (1) and considering the mesoscopic leads to be unpolarizable, we get

$$\frac{\mathrm{d}\theta_\mathrm{f}}{\mathrm{d}E} \approx \pi[\rho^{(W)}(E) - \rho_0^{(W)}(E)]. \tag{16}$$

The non-polarizability here means that the last three terms on the RHS of equation (13) are to be ignored. Actually even if one does not want to invoke the non-polarizability of the leads, one can evaluate the last three integrals and see that these terms are negligibly small in the regime of interest, which is the WKB regime. This is the regime where transport occurs. For example, the WKB regime for such constant potentials occurs for $E > V$. In this regime, $|R_{11}|$ or $|R_{22}|$ or $|R_{33}|$ is an order of magnitude smaller than v (note that the factor h is present in all the terms on the RHS of equation (13) and the integrands in the last three terms of equation (13) are oscillatory functions and the integrations are smaller than 1).

4. Determination of $\rho_0^{(W)}(E)$

Note that in the LHS of equation (16), one has to consider the absolute scattering phase shifts (and not phase shifts relative to phase shifts in absence of scattering), and on the RHS $\rho^{(W)}(E)$ is the DOS in the system in the presence of scattering, and $\rho_0^{(W)}(E)$ is that in the absence of scattering. One can have alternate formalisms, wherein one considers the relative phase shifts on the LHS but all these are equivalent. If one works out the FSR in one particular formalism, what its form will be in another formalism is obtained by simple algebra. So we shall consider absolute phase shifts on the LHS because they can be defined for any system. $\rho^{(W)}(E)$ also can be defined for any system. But it is not clear what the DOS is in the absence of scattering in the case of scattering by topological structures as in the present case. It is known that for such topological structures there may not be any continuous way of going to the situation where there is no scattering.

For example, in case of the three-prong potential, it is not possible to realize the state of 'absence of scattering'. Even if we make the potential V in figure 1 continuously go to 0, we get $T_{12} = T_{13} = 2/3$ and $R_{11} = -1/3$ for $l_1 = l_2 = l_3$. Naturally, this is true also for unequal l_1, l_2 and l_3, since with zero potential there is no reflection at points A, C, and D. Nevertheless, the result for $V = 0$ provides us with a way to solve $\rho_0^{(W)}$.

In the case of $V = 0$ we write

$$\frac{\mathrm{d}\theta'_\mathrm{f}}{\mathrm{d}E} \approx \pi[\rho^{(W')}(E) - \rho_0^{(W)}(E)] \tag{17}$$

where W' stands for the thick region in figure 1 with V set to 0. θ' is calculated from the S matrix when $V = 0$, while $\rho_0^{(W)}(E)$ is independent of the scattering potential V. The corresponding S matrix becomes

$$S' = \begin{pmatrix} -(1/3)\mathrm{e}^{2\mathrm{i}kl_1} & (2/3)\mathrm{e}^{2\mathrm{i}kl_2} & (2/3)\mathrm{e}^{2\mathrm{i}kl_3} \\ (2/3)\mathrm{e}^{2\mathrm{i}kl_1} & -(1/3)\mathrm{e}^{2\mathrm{i}kl_2} & (2/3)\mathrm{e}^{2\mathrm{i}kl_3} \\ (2/3)\mathrm{e}^{2\mathrm{i}kl_1} & (2/3)\mathrm{e}^{2\mathrm{i}kl_2} & -(1/3)\mathrm{e}^{2\mathrm{i}kl_3} \end{pmatrix} \tag{18}$$

where all matrix elements have their absolute phases. Using equation (2) we get

$$\frac{\mathrm{d}\theta'_\mathrm{f}}{\mathrm{d}E} = \frac{\mathrm{d}}{\mathrm{d}E}\left(\frac{1}{2\mathrm{i}}\log \mathrm{Det}[S']\right) = 2\pi\left(\frac{l_1}{hv} + \frac{l_2}{hv} + \frac{l_3}{hv}\right). \tag{19}$$

On the other hand, we can calculate $\rho^{(W')}$ directly using equations (14) and (15), with solutions of equations (6)–(11). A straightforward derivation gives

$$\rho^{(W')}(E) = \frac{2l_1}{hv} + \frac{2l_2}{hv} + \frac{2l_3}{hv}. \tag{20}$$

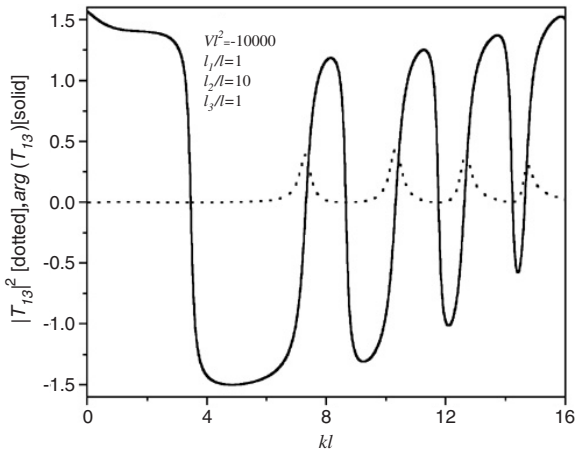

Figure 2. arg(T_{13}) (solid curve) decreases sharply but continuously, when $|T_{13}|^2$ (dotted curve) minimizes. This is a signature of multichannel Fano resonance. l is the unit of length.

Substituting (19) and (20) in equation (17) gives

$$\rho_0^{(W)}(E) = 0. \tag{21}$$

Since $\rho_0^{(W)}(E)$ is independent of depth of the potential V we get from equation (16)

$$\frac{\mathrm{d}\theta_\mathrm{f}}{\mathrm{d}k} \approx \hbar v \rho^{(W)}(k) \tag{22}$$

where we have made a change of variable from E to wavevector k. So although at first it was not clear how to define $\rho_0^{(W)}(E)$ when we cannot realize the state of absence of scattering, we have finally obtained that it is no different from a 1D situation. This is because the S-matrix elements of the three-prong potential for $V \to 0$ do not have any non-trivial energy dependence (the energy dependence is the same as that of a free particle, i.e., of the form $\mathrm{e}^{\mathrm{i}kl}$). Note that the above method can also be used for more complicated junctions.

5. Results and discussions

We first show that the three-prong potential can exhibit multichannel Fano resonance. In figure 2, we show that arg(T_{13}) drops sharply when $|T_{13}|^2$ minimizes. In figure 3, we show that arg(R_{11}) drops sharply when $|R_{11}|^2$ minimizes. These are typical signatures of Fano resonances [13]. Exactly similar behaviour has been obtained in the experiments of Kobayashi *et al* [6, 7]. Since these phase shifts can be detected experimentally, it is important to investigate the physical information that can be obtained from such phase shifts. In the following we will show that arg(T_{12}) does not show any drop and also calculate the DOS explicitly to check if the DOS and the Friedel phase are related to arg(T_{12}). Our previous experience, as discussed in section 2, suggests that this could be the case.

In figure 4, we plot $\frac{\mathrm{d}}{\mathrm{d}(kl)}$ arg(T_{12}) as a function of kl. It shows sharp peaks and is positive everywhere, implying that unlike in arg(T_{13}) or arg(R_{11}), there are no drops or negative slopes in arg(T_{12}). Also $\frac{\mathrm{d}}{\mathrm{d}(kl)}$ arg(T_{12}) is very close to $\frac{\mathrm{d}\theta_\mathrm{f}}{\mathrm{d}(kl)}$ and $\hbar v \rho^{(W)}(kl)$. Here l is taken to be the unit of length. However, unlike the case of the δ function potential in quasi-1D, $\frac{\mathrm{d}}{\mathrm{d}(kl)}$ arg(T_{12}) is not identical to $\frac{\mathrm{d}\theta_\mathrm{f}}{\mathrm{d}(kl)}$. Nevertheless they are indeed very close to each other and identical

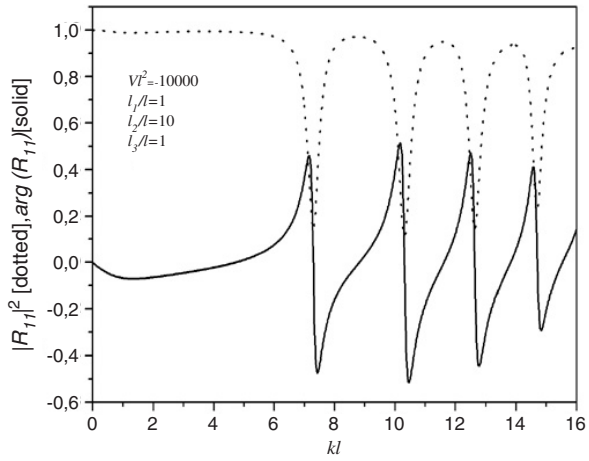

Figure 3. $\arg(R_{11})$ (solid curve) decreases sharply but continuously, when $|R_{11}|^2$ (dotted curve) minimizes. This is a signature of multichannel Fano resonance. l is the unit of length.

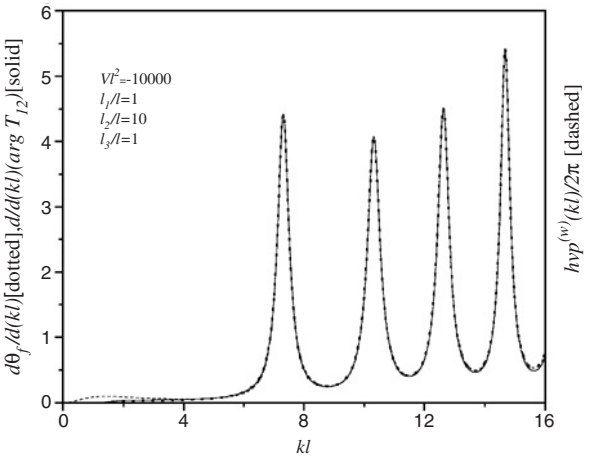

Figure 4. $\frac{\mathrm{d}}{\mathrm{d}(kl)}\arg(T_{12})$ (solid curve) is positive everywhere, implying that there are no negative slopes in $\arg(T_{12})$. $\frac{\mathrm{d}}{\mathrm{d}(kl)}\arg(T_{12})$ (solid curve) and $\frac{\mathrm{d}\theta_\mathrm{f}}{\mathrm{d}(kl)}$ (dotted curve) are very close to each other, implying that $\arg(T_{12})$ should carry all the information about the DOS. Explicit calculations of $\hbar v\rho^{(W)}(kl)$ (dashed curve) confirm this. l is the unit of length.

for practical purposes when the Fano resonances are long lived (the coupling to the leads is weak and the resonances are very sharp). This is usually what is seen in quantum dot experiments [6, 7]. However, for Fano resonances with short life times, there are quantitative differences, although there is qualitative similarity, as shown in figure 5. In figure 6, we consider a shorter value for the length l_2. As a result, along with the Fano resonances, there are also some Breit–Wigner resonances. The resonances due to multiple scattering between A and B (or between B and C) are Breit–Wigner resonances, while those due to multiple scattering between B and D are Fano resonances. All these resonances are clearly characterized by a peak in the DOS. All of them are long lived resonances as we are using a large value for V. $\frac{\mathrm{d}}{\mathrm{d}(kl)}\arg T_{12}$ gives all these peaks qualitatively and quantitatively for the Fano resonances. But

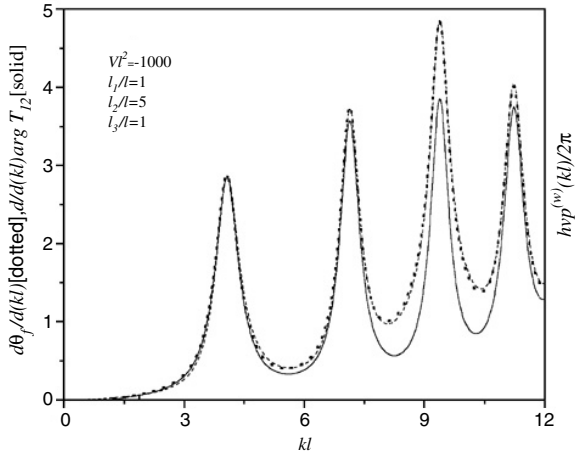

Figure 5. Here we plot the same things as in figure 4. The difference is that the resonances are short lived as compared to those in figure 4. The peaks in $\hbar v\rho^{(W)}(kl)$ are broader as compared to those in figure 4. $\frac{\mathrm{d}}{\mathrm{d}(kl)}\arg(T_{12})$ is qualitatively similar to $\frac{\mathrm{d}\theta_f}{\mathrm{d}(kl)}$ or $\hbar v\rho^{(W)}(kl)$. There are quantitative differences.

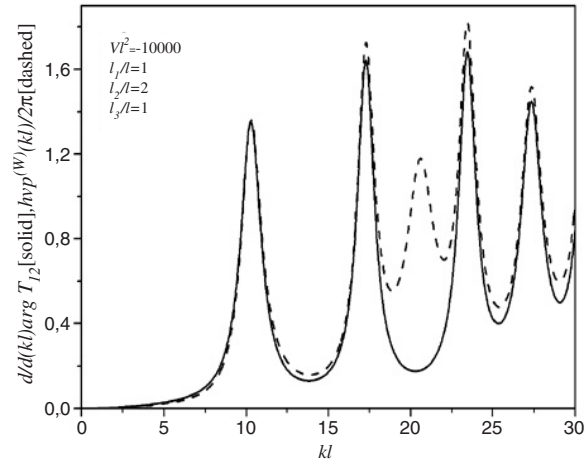

Figure 6. Here we plot the same things as in figure 4. The difference is that l_2 is much shorter compared to those in figure 4. Except for the third resonance, all the resonances are Fano resonances. $\frac{\mathrm{d}}{\mathrm{d}(kl)}\arg(T_{12})$ is quantitatively similar to $\hbar v\rho^{(W)}(kl)$ only at the Fano resonances.

it completely misses the third resonance, which is a Breit–Wigner resonance. On can check with different parameter values that the DOSs at the Fano resonances are correctly given by $\frac{\mathrm{d}}{\mathrm{d}(kl)}\arg T_{12}$, but at the Breit–Wigner resonances they are not.

6. Conclusions

Fano resonances occur very frequently in mesoscopic systems. Not much is known about scattering phase shifts for Fano resonances. We show that the three-prong potential is a simple model that gives multichannel Fano resonance. Unlike previously studied potentials that show Fano resonances, this is an extended potential. In the case of Fano resonances, scattering

phase shifts in only some particular channels show sharp phase drops while others do not. The channels that do not show the phase drops seem to be the more informative channels and hence very special channels. It seems that the DOS is related to the scattering phase shifts of these special channels. As this is exact for point scatterers, we were tempted to check it for an extended scatterer that exhibited Fano resonance. The three-prong potential studied shows that this is true when the Fano resonances are long lived. In all the experiments so far [6, 7, 15] one has encountered long lived Fano resonances where the phase drops are very sharp. As the life time of the resonances decreases, the energy derivative of the scattering phase shifts in these special channels and integrated charge inside the scatterer start deviating from each other. However, they are qualitatively similar. For Breit–Wigner resonances, there is not even qualitative agreement between them. The phase shift in the channels that exhibit the phase drops do not give any information about the DOS, qualitatively or quantitatively, for long lived resonances or short lived resonances. So far, experiments [6, 7, 15] and theories [9, 14] have mostly focused on the phase shifts of these non-informative channels. We hope that this will give some clues to future works to find a mathematical proof of this fact. Such a proof should be consistent with the features observed in the three-prong potential and in the δ function potential in a quantum wire.

References

[1] Datta S 1995 *Electronic Transport in Mesoscopic Systems* (Cambridge: Cambridge University Press)
[2] Gangopadhyay A, Pagnamenta A and Sukhatme U 1995 *J. Phys. A: Math. Gen.* **28** 5331
Buttiker M, Imry Y and Azbel M Ya 1984 *Phys. Rev.* A **30** 1982
[3] Deo P S 1996 *Phys. Rev.* B **53** 15447
[4] Pascaud M and Montambaux G 1999 *Phys. Rev. Lett.* **82** 4512
Anda E V, Busser C, Chiappe G and Davidovich M A 2002 *Phys. Rev.* B **66** 035307
Buttiker M and Stafford C A 1996 *Phys. Rev. Lett.* **76** 495
Cho S Y, Kang K, Kim C K and Ryu C M 2001 *Phys. Rev.* B **64** 033314
[5] Voo K-K, Chen S-C, Tang C-S and Chu C-S 2006 *Phys. Rev.* B **73** 35307
[6] Kobayashi K, Aikawa H, Katsumoto S and Iye Y 2003 *Phys. Rev.* B **68** 235304
[7] Kobayashi K, Aikawa H, Sano A, Katsumoto S and Iye Y 2004 *Phys. Rev.* B **70** 035319
[8] Deo P S 2000 *Preprint* cond-mat/0005123
[9] Yeyati A L and Buttiker M 2000 *Phys. Rev.* B **62** 7307
[10] Aharony A, Entin-Wohlman O and Imry Y 2003 *Preprint* cond-mat/0308414
Entin-Wohlman O, Aharony A, Imry Y, Levinson Y and Schiller A 2002 *Phys. Rev. Lett.* **88** 166801
[11] Akkermans E, Auerbach A, Avron J E and Shapiro B 1991 *Phys. Rev. Lett.* **66** 76
[12] Das M P and Green F 2003 *J. Phys.: Condens. Matter* **15** L687
[13] Bandopadhyay S and Deo P S 2003 *Phys. Rev.* B **68** 113301
Deo P S, Bandopadhyay S and Das S 2002 *Int. J. Mod. Phys.* B **16** 2247
[14] Taniguchi T and Buttiker M 1999 *Phys. Rev.* B **60** 13814
[15] Schuster R *et al* 1997 *Nature* **385** 417
[16] Yeyati A L and Buttiker M 1995 *Phys. Rev.* B **52** R14360
[17] Deo P S 1998 *Solid State Commun.* **107** 69
[18] Deo P S, Koskinen P and Manninen M 2005 *Phys. Rev.* B **72** 155332
[19] D'Amato J L, Pastawaski H M and Weisz J F 1989 *Phys. Rev.* B **39** 3554
[20] Voo K-K and Chu C S 2005 *Phys. Rev.* B **72** 165307
[21] Nockel J U and Stone A D 1994 *Phys. Rev.* B **50** 17415
[22] Lee H-W 1999 *Phys. Rev. Lett.* **82** 2358
[23] Madhavan *et al* 1998 *Science* **280** 567
Rotter *et al* 2004 *Phys. Rev.* E **69** 046208
[24] Harrison W A 1979 *Solid State Theory* (New York: Dover)
[25] Shao *et al* 1994 *Phys. Rev.* B **49** 7453